# Effective-medium theories for two-phase dielectric media

A. N. Norris, P. Sheng, and A. J. Callegari

Exxon Research and Engineering Company, Corporate Research Science Laboratories, Route 22 East, Clinton Township, Annandale, New Jersey 08801

(Received 4 September 1984; accepted for publication 31 October 1984)

Two different effective-medium theories for two-phase dielectric composites are considered. They are the effective medium approximation (EMA) and the differential effective medium approximation (DEM). Both theories correspond to realizable microgeometries in which the composite is built up incrementally through a process of homogenization. The grains are assumed to be similar ellipsoids randomly oriented, for which the microgeometry of EMA is symmetric. The microgeometry of DEM is always unsymmetric in that one phase acts as a backbone. It is shown that both EMA and DEM give effective dielectric constants that satisfy the Hashin-Shtrikman bounds. A new realization of the Hashin-Shtrikman bounds is presented in terms of DEM. The general solution to the DEM equation is obtained and the percolation properties of both theories are considered. EMA always has a percolation threshold, unless the grains are needle shaped. In contrast, DEM with the conductor as backbone always percolates. However, the threshold in EMA can be avoided by allowing the grain shape to vary with volume fraction. The grains must become needlelike as the conducting phase vanishes in order to maintain a finite conductivity. Specifically, the grain-shape history for which EMA reproduces DEM is found. The grain shapes are oblate for low-volume fractions of insulator. As the volume fraction increases, the shape does not vary much, until at some critical volume fraction there is a discontinuous transition in grain shape from oblate to prolate. In general, it is not always possible to map DEM onto an equivalent EMA, and even when it is, the mapping is not preserved under the interchange of the two phases. This is because DEM is inherently unsymmetric between the two phases.

#### I. INTRODUCTION

We discuss the effective-medium problem in the context of a two-phase dielectric medium. The emphasis will be on comparing two widely used but apparently dissimilar theories, the effective-medium approximation and the differential-effective-medium theory. Recently, <sup>1,2</sup> it has been shown that both theories are realizable in terms of homogenization processes. The homogenization is defined by building up the final material incrementally from some starting material. In this paper, we discuss the similarities and differences of the two theories, with emphasis on percolation properties and bounds. We show in another paper that both theories are special cases of a wider class of homogenization processes.<sup>3</sup>

The effective-medium approximation (EMA)<sup>4-8</sup> is also known as the self-consistent approximation, the coherent-potential approximation (CPA), and Bruggeman's theory, among various other names. The idea in EMA is to embed an isolated inclusion of material 1 in a homogeneous medium with dielectric constant  $\epsilon$ . The depolarization field due to the inclusion in the presence of an external field is calculated. The depolarization field due to a similar inclusion of material 2 is also calculated and  $\epsilon$  is determined by requiring that the average depolarization field of the two inclusions equal zero. EMA may also be defined dynamically by requiring the average forward-scattering amplitudes of the inclusions to cancel in the low-frequency limit. 9,10

It is possible to define a class of realizable microgeometries for which EMA gives the exact solution. These media are defined by a specific homogenization process. Basically, the idea is to start with a medium having permittivity  $\epsilon_0$ . With this as a host, grains of materials 1 and 2 are embedded

so that they are well separated and occupy a very-smallvolume fraction of the new medium. The relative volume fractions of the dilute suspension are  $f_1$  and  $f_2$ . In the next step, grains large relative to the previous grains are embedded. The process is repeated such that at each step the new grain sizes are large relative to the previous ones and the relative volume fractions  $f_1$  and  $f_2$  are always adhered to. A limiting process is defined such that the ratio of the relative sizes at each step become infinite, while the number of steps tend to infinity. The resultant material has effective properties defined by EMA. A rigorous proof of this identity has been given by Milton. 11 The above process may be thought of as one of continuous homogenization. At each step we are replacing an infinitesimal amount of material by the same amount of materials  $\epsilon_1$  and  $\epsilon_2$ . The new material is then homogenized and the process is repeated until all of the original material is replaced. Thus, it is irrelevant what the initial properties  $\epsilon_0$  are.

Differential-effective—medium theory (DEM)<sup>2,12–15</sup> is also defined by homogenization. Other names for DEM include: the self-similar effective—medium approximation, the granular-effective-medium approximation, and the iterated-dilute approximation. Beginning with pure material 1, an infinitesimal amount of material 2 is added, such that each grain of material 2 is a similarly shaped ellipsoid with arbitrary orientation. The mixture is then homogenized and the process repeated until the volume fraction of material 2 in the composite equals  $f_2$ . Thus, unlike EMA, the starting material is not completely replaced.

Both EMA and DEM have been used in estimating the effective properties of two-phase composites. EMA is gener-

ally used for symmetric configurations, while DEM is used for materials in which one phase always percolates, e.g., water in rock with the water always connected.<sup>2,12</sup>

The question about the accuracy of the various effective-medium theories has often been raised. This is particularly the case when different EM theories produce differing predictions about the physical characteristics of a "random composite." In the past several years, it has become increasingly clear that while the microstructure i.e., the topological arrangements and shapes of the grains, is usually not explicitly considered in the derivation of EM theories, each EM theory nevertheless implies a definite type of underlying structure for the random composite. Therefore, the real question should be, "How accurate is the EM theory in describing the physical properties of its implied structure?" While a complete answer to this question is difficult, in certain cases we see that an EM theory is associated with an exactly realizable microgeometry. In these cases, the EM theories are, of course, exact (for the particular structure). Yet the same theory would be in error when considered in respect to a different microstructure. It would be meaningful, therefore, to turn the question around and ask, "How accurate is the microstructure in describing the effective medium theory?"

## II. EFFECTIVE-MEDIUM APPROXIMATION

Let  $\epsilon_1$  and  $\epsilon_2$  be the complex dielectric constants of the two constituents and let  $f_1$  and  $f_2 = 1 - f_1$  be their respective volume fractions. Let  $\epsilon$  be the effective permittivity of the composite mixture. The two components are distributed in space with definite distributions of geometrical shapes and sizes of the particles. In EMA, the size of the particles is not important, provided that they are small compared with the wavelength of the probing wave; all we need to specify are the distributions of shapes. We take the shapes to be ellipsoids which are randomly oriented in space. In addition, we assume that each component has only one particular shape, and that the shape is the same for both materials. In other words, the shape distribution is a delta function. The ellipsoids are described by the depolarization coefficients  $L_i$ , i = 1, 2, and 3 for the 3 major axes of the ellipsoid (see Landau and Lifshitz<sup>16</sup>). The L's are all positive and satisfy

$$L_1 + L_2 + L_3 = 1. (1)$$

For spheres,  $L_1 = L_2 = L_3 = 1/3$  and for circles,  $L_1 = L_2 = 1/2$  and  $L_3 = 0$ . A spheroid has two L's equal. As  $L \rightarrow 0$ , the associated major axis becomes infinitely long and as  $L \rightarrow 1$  the major axis shrinks to zero relative to the other major axes. A needle corresponds to the limit  $L_1 \rightarrow 0$ ,  $L_2 \rightarrow 1/2$ ,  $L_3 = 1/2$ ; a plate or disk corresponds to  $L_1 \rightarrow 0$ ,  $L_2 \rightarrow 0$ ,  $L_3 \rightarrow 1$ . The general relationship between the L's and the aspect ratios of the ellipsoid are given, for example, in Landau and Lifshitz<sup>16</sup> or Mendelson and Cohen. The EMA then predicts  $\epsilon$ , where  $\epsilon$  solves the following equation,

$$\sum_{i=1,3} \left( \frac{f_1(\epsilon - \epsilon_1)}{(1 - L_i)\epsilon + L_i\epsilon_1} + \frac{f_2(\epsilon - \epsilon_2)}{(1 - L_i)\epsilon + L_i\epsilon_2} \right) = 0, \quad (2)$$

which can be rewritten

$$\sum_{i=1,3} \frac{1}{(1-L_i)^2} \left( \frac{f_1}{\epsilon + D_i \epsilon_1} + \frac{f_2}{\epsilon + D_i \epsilon_2} \right) = \sum_{i=1,3} \frac{1}{1-L_i},$$
(3)

where

$$D_i = L_i / (1 - L_i). \tag{4}$$

In general, the EMA equation has 6 roots. It is clear from Eq. (3) that if  $\epsilon_1$  and  $\epsilon_2$  are real, then all the roots are real. There are five negative roots interlaced between the 6 points  $-\epsilon_1 D_i$  and  $-\epsilon_2 D_i$ , i=1,3. The remaining root is positive and is the EMA root. If we generalize to the case where the two materials have different shaped grains, then the depolarization coefficients are different for each material and this must be included in the EMA equation. However, the basic properties are unchanged, and there is still only one positive root. We show in Appendix A that this root always lies within the Hashin-Shtrikman bounds. However, since keeping the shapes the same results in a symmetric theory, and also reduces the algebra, we focus our attention on the symmetric EMA defined by Eq. (2).

When  $\epsilon_2 \rightarrow 0$ , three of the roots collapse onto zero. Whether or not the physical root is one of these zeroes depends upon  $f_2 \equiv \phi$ . There is a critical value of  $\phi$  at  $\phi_c$ , called the percolation threshold, below which the physical root is greater than zero. However, when  $\phi \geqslant \phi_c$  there is no positive root and so  $\epsilon = 0$ . For  $\phi < \phi_c$  we have  $\epsilon = \gamma \epsilon_1$ , where  $\gamma$  is the positive root of the cubic equation

$$\sum_{i=1,3} \frac{1}{1 - L_i} \left( \frac{1 - \phi}{L_i + \gamma (1 - L_i)} - \frac{1 - \phi_c}{L_i} \right) = 0, \quad (5)$$

and

$$\phi_c = \frac{\sum 1/L_i}{\sum 1/L_i + \sum 1/(1 - L_i)}.$$
 (6)

It may be shown that  $2/3 \le \phi_c \le 1$ , and the minimum is achieved when  $L_1 = L_2 = L_3 = 1/3$ , i.e., when the grains are spheres, the maximum is achieved if one of the  $L_i \rightarrow 0$ , which corresponds to needles. Therefore, there is no percolation threshold for needle-shaped particles.

The above results simplify when the grain shape reduces to a spheroid. Let  $L_1 = L$ ,  $L_2 = L_3 = (1 - L)/2$ , then we have

$$\phi_c = \frac{(1+L)(1+3L)}{1+9L}. (7)$$

We note that L < 1/3 for prolate spheroids, and L > 1/3 for oblate spheroids, respectively. The EMA solution for  $\epsilon_2 = 0$  is given by  $\epsilon = 0$  for  $\phi = f_2 > \phi_c$  and is  $\epsilon = \gamma \epsilon_1$  for  $\phi < \phi_c$ , where  $\gamma$  is the positive root of the quadratic equation

$$(1 - \phi)(\gamma - 1) \left( \frac{1}{(1 - L)\gamma + L} + \frac{4}{(1 + L)\gamma + (1 - L)} \right) + \phi \frac{5 - 3L}{1 - L^2} = 0.$$
 (8)

We have plotted  $\gamma(\phi)$  in Figs. 1 and 2 for prolate and oblate spheroids, respectively. We note the range of  $\gamma$  for  $\phi < 4/9$  is much less for prolate spheroids than for oblate spheroids. The range of attainable  $\gamma$  is bounded above by the union of the L=1/3 and L=0 curves. Thus,  $\gamma < 1-(3/2)\phi$  for  $0<\phi<4/9$ , and  $\gamma<\{4-9\phi+[(4-9\phi)^2+20(1-\phi)]^{1/2}\}/$ 

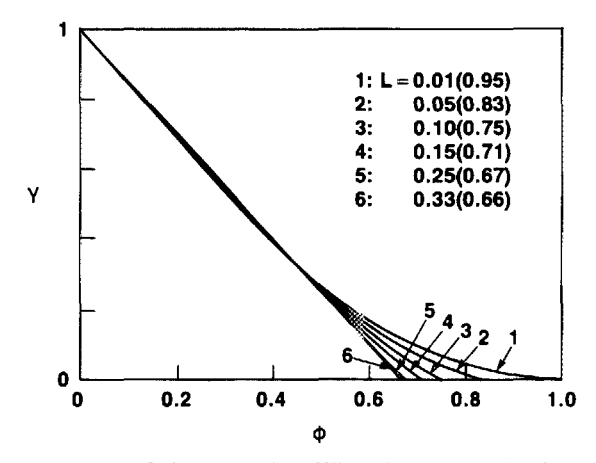


FIG. 1. Percolation properties of EMA for prolate spheroids, 0 < L < 1/3. The percolation threshold  $\phi_c$  is given in brackets for each value of L.

10 for  $4/9 < \phi < 1$ . As  $L \rightarrow 0$ , the percolation threshold goes to unity. However, the maximum percolation threshold for oblate spheroids is 0.8, which is attained by plates (L = 1).

#### III. DIFFERENTIAL-EFFECTIVE-MEDIUM THEORY

The derivation of DEM is based upon the low-concentration expansion of EMA, or of any theory which is correct to first order in  $\phi \equiv f_2$  as  $\phi \rightarrow 0$ . We have, from Eq. (2)

$$\epsilon = \epsilon_1 - g(\epsilon_1, \epsilon_2)\phi + O(\phi^2), \tag{9}$$

where

$$g(\epsilon, \epsilon_2) = \frac{1}{3} \sum_{i=1,3} \frac{\epsilon(\epsilon - \epsilon_2)}{\epsilon(1 - L_i) + L_i \epsilon_2}.$$
 (10)

Thus, at  $\phi = 0$  we have  $\epsilon = \epsilon_1$  and

$$\epsilon' = -g(\epsilon, \epsilon_2), \tag{11}$$

where the prime denotes differentiation with respect to  $\phi$ . We now view Eq. (12) as defining a differential process for all values of  $\phi$  between 0 and 1. However, it is necessary to include a volume correction term for  $\phi$  nonzero. We do this by multiplying the right-hand side of Eq. (11) by a volume correction factor  $1/(1-\phi)$ . We then have the following initial value problem for  $\epsilon(\phi)$ :

$$\epsilon' = \frac{-g(\epsilon, \epsilon_2)}{1 - \phi}, \quad \epsilon(0) = \epsilon_1,$$
 (12)

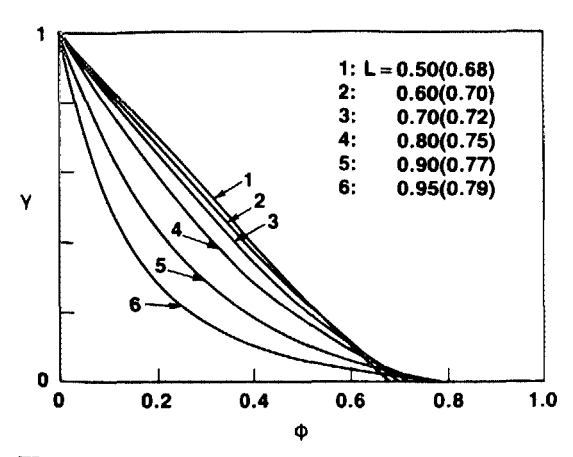


FIG. 2. Percolation properties of EMA for oblate spheroids.

which integrates to give the implicit solution

$$1 - \phi = \left(\frac{\epsilon_1}{\epsilon}\right)^{R(0)} \left(\frac{\epsilon - \epsilon_2}{\epsilon_1 - \epsilon_2}\right) \left(\frac{\epsilon_1 - \gamma_1 \epsilon_2}{\epsilon - \gamma_1 \epsilon_2}\right)^{R(\gamma_1)} \times \left(\frac{\epsilon_1 - \gamma_2 \epsilon_\epsilon}{\epsilon - \gamma_2 \epsilon_2}\right)^{R(\gamma_2)}.$$
 (13)

Here  $\gamma_1$  and  $\gamma_2$  are the two negative roots of  $g(\gamma,1)=0$ . Assuming that  $L_1>L_2>L_3$ , then one of the roots is between  $-D_1$  and  $-D_2$  and the other between  $-D_2$  and  $-D_3$ , where  $D_1, D_2$ , and  $D_3$  are defined in Eq. (4). The function  $R(\gamma)$  is defined as

$$R(\gamma) = -\left[\frac{dg}{d\gamma}(\gamma,1)\right]^{-1}.$$
 (14)

Therefore,  $R(\gamma_1)$ ,  $R(\gamma_2)>0$  and we have

$$R(0) = \left(\sum \frac{1}{3L_i}\right)^{-1}.$$
 (15)

Thus, 0 < R(0) < 1/3 with R(0) = 1/3 for spheres and R(0) = 0 for needles or plates. The following relation can be derived using residue calculus;

$$R(\gamma_1) + R(\gamma_2) = 1 - \left(\sum \frac{1}{3(1 - L_i)}\right)^{-1} - \left(\sum \frac{1}{3L_i}\right)^{-1}.$$
(16)

Thus,

$$1 \geqslant R(\gamma_1) + R(\gamma_2) \geqslant 0, \tag{17}$$

and the lower bound is achieved by spheres, the upper bound by plates. We also note that  $\gamma_1$  and  $\gamma_2$  satisfy

$$(1 - 4\gamma_1)(1 - 4\gamma_2) = 9. (18$$

This relation is independent of the values of  $L_1$ ,  $L_2$ , and  $L_3$ , and implies that  $\gamma_1$  and  $\gamma_2$  lie on either side of -1/2. We show in Appendix A that the solution to Eq. (13) always satisfies the Hashin-Shtrikman bounds.

The result in Eq. (13) simplifies considerably if the grain shape reduces to a spheroid. Then one of  $R(\gamma_1)$  and  $R(\gamma_2)$  is zero. Without loss of generality we take  $R(\gamma_2) = 0$ . Then

$$\gamma_1 = -(1+3L)/(5-3L), \tag{19}$$

and  $R(\gamma_1)$  follows from Eq. (16). The general solution simplifies in the three limiting cases of spheres, needles, and plates. For spheres, we have

$$1 - \phi = \left(\frac{\epsilon - \epsilon_2}{\epsilon_1 - \epsilon_2}\right) \left(\frac{\epsilon_1}{\epsilon}\right)^{1/3},\tag{20}$$

while for needles,

$$1 - \phi = \left(\frac{\epsilon - \epsilon_2}{\epsilon_1 - \epsilon_2}\right) \left(\frac{5\epsilon_1 + \epsilon_2}{5\epsilon + \epsilon_2}\right)^{2/5},\tag{21}$$

and for plates (disks),

$$1 - \phi = \left(\frac{\epsilon - \epsilon_2}{\epsilon_1 - \epsilon_2}\right) \left(\frac{\epsilon_1 + 2\epsilon_2}{\epsilon + 2\epsilon_2}\right). \tag{22}$$

An explicit expression for  $\epsilon$  can be obtained only in the case of plates. From Eq. (22), we find that  $\epsilon = h(\epsilon_2)$ , where the function h is defined in Eq. (A1). Therefore, it follows from the results of Appendix A, specifically Eqs. (A1) and (A2), that  $\epsilon$  for plates equals the lower Hashin-Shtrikman bound if  $\epsilon_1 > \epsilon_2$  and the upper bound otherwise. It is well known that the Hashin-Shtrikman bounds both correspond to spe-

cific packed coated-spheres microgeometries.<sup>17</sup> Another realization of these bounds is thus possible through DEM with platelike grains.

We now consider the case when the added phase is insulating. Putting  $\epsilon_2 = 0$ , we obtain from Eqs. (13), (15), and (16) the simple result

$$\epsilon = \epsilon_1 (1 - \phi)^m, \tag{23}$$

where

$$m = \frac{1}{3} \sum_{i=1,3} \frac{1}{1 - L_i} \,. \tag{24}$$

The form of Eq. (23) agrees with Archie's law  $\sigma = \sigma_f p^m$  for the conductivity of porous rock, where  $\sigma$  is the conductivity of the rock,  $\sigma_f$  the conductivity of the pore fluid, p is the porosity, and  $m \approx 2$  a constant. From Eq. (24), we see that  $m \geqslant 3/2$ , with equality for spheres,  $m \rightarrow \infty$  for plates, and for an arbitrary sperhoid

$$m = \frac{5 - 3L}{3(1 - L^2)} \,. \tag{25}$$

However, Eq. (23) must be used with caution as  $m \to \infty$ , i.e., as the grains become platelike. Equation (23) was derived after taking the limit  $\epsilon_2 \to 0$ . The further limit  $m \to \infty$  must be handled carefully. For  $\epsilon_2 > 0$ , consider the limit of oblate spheroidal grains that become platelike. As  $m \to \infty$ , we have  $L \sim 1$  from Eq. (25), so that from Eq. (19)  $\gamma_1 \sim -2$ . Also, from Eqs. (13) and (16) we have  $R(0) \sim 1/(4m)$ ,  $R(\gamma_1) \sim 1 - 5/(4m)$ , so that

$$1 - \phi \sim \left(\frac{\epsilon_1}{\epsilon}\right)^{1/4m} \left(\frac{\epsilon - \epsilon_2}{\epsilon_1 - \epsilon_2}\right) \left(\frac{\epsilon_1 + 2\epsilon_2}{\epsilon + 2\epsilon_2}\right)^{(1 - 5/4m)}. \tag{26}$$

Now as we let  $\epsilon_2 \rightarrow 0$  we see two types of solution. The first is valid for  $(1 - \phi)^m > \epsilon_2/\epsilon_1$  and is

$$\epsilon \sim \epsilon_1 (1 - \phi)^m$$

which is the same as Eq. (23). Note that if  $\phi$  is not near 0 or 1, the condition  $(1 - \phi)^m > \epsilon_2/\epsilon_1$  is equivalent to  $m < \ln(\epsilon_1/\epsilon_2)$ . The second type of solution occurs when  $m > \ln(\epsilon_1/\epsilon_2)$ , in which case we get

$$\epsilon \sim \epsilon_2 (3 - 2\phi)/\phi$$
.

1993

This is just the Hashin-Shtrikman lower bound given by Eq. (22) with  $\epsilon_2/\epsilon_1 < 1$ .

The Hashin-Shtrikman upper bound for a conductor-insulator composite is

$$\epsilon = \epsilon_1 [2(1 - \phi)/(2 + \phi)]. \tag{27}$$

We claimed above that this is realizable through DEM with the embedded phase in the shape of disks. Therefore, to achieve the upper bound we must alter the roles of  $\epsilon_1$  and  $\epsilon_2$ . Again, we must be careful in taking the dual limits  $\epsilon_2 \rightarrow 0$ ,  $m \rightarrow \infty$ . A blind application of the DEM equations with an insulating matrix would suggest a composite that is always insulating. However, putting  $\epsilon_2 > 0$ , and letting  $m \rightarrow \infty$ , we derive in the same manner as Eq. (26) the result

$$\phi \sim \left(\frac{\epsilon_2}{\epsilon}\right)^{1/4m} \left(\frac{\epsilon - \epsilon_1}{\epsilon_2 - \epsilon_1}\right) \left(\frac{\epsilon_2 + 2\epsilon_1}{\epsilon + 2\epsilon_1}\right)^{(1 - 5/4m)}.$$

As  $\epsilon_2 \rightarrow 0$ , the solution to this equation equals the Hashin-Shtrikman upper bound if

$$(\epsilon_2/\epsilon_1)^{1/4m} \sim 1$$
,

or alternatively, if

$$m > (1/4) \ln(\epsilon_1/\epsilon_2)$$
.

This relation tells us how disklike the conducting grains must be as  $\epsilon_2 \rightarrow 0$ .

The DEM equation (12) can be generalized to include distributions of shapes  $^{12}$  and shapes which vary with concentration. As the latter possibility has not been discussed previously, we consider it briefly here. For simplicity, assume the inclusion shape to be spheroidal such that  $L = L(\phi)$ . In addition, let  $\epsilon_2 = 0$ , then the variable-L version of Eq. (12) becomes

$$\epsilon' = -m(\phi)\epsilon/(1-\phi), \quad \epsilon(0) = \epsilon_1,$$
 (28)

where  $m = m(\phi)$  follows from Eq. (25) with L as a function of  $\phi$ . Equation (28) gives the Archies-law result of Eq. (23) when m is constant. Simple examples of  $m(\phi)$  are presented in Table I. We note that  $\epsilon(\phi)$  behaves as  $(1 - \phi)^{m(1)}$  as  $\phi \to 1$  if m is bounded at  $\phi = 1$ . A finite percolation threshold results from an infinity of  $m(\phi)$  for  $\phi < 1$ . This happens because  $L \to 1$  as  $m \to \infty$ , which means the insulator becomes platelike, and hence the effective conductivity goes to zero. The fourth example of Table I gives the Hashin-Shtrikman upper bound for a conductor-insulator composite. However, the m is unphysical, since it is less than 3/2.

### IV. INTERPRETATION OF DEM IN TERMS OF EMA

Consider the percolation problem for  $\epsilon_2 = 0$ . We saw that EMA has a finite percolation threshold for fixed grain shape, while DEM always has a zero percolation threshold. However, it is possible to avoid the percolation threshold in EMA by allowing the grain shape to vary as a function of  $\phi$ . In this section, we consider EMA for spheroids where the depolarization L is allowed to vary with volume fraction. In particular, we consider the set of  $L(\phi)$  which map EMA onto the DEM solution of Eq. (23) for fixed m. The object of the exercise is to compare one realizable effective-medium theory with another. The associated microgeometry of DEM is characterized by a "backbone" of material, in our case material 1, the conductor. The EMA microgeometry consists of similarly shaped grains of either material. There is no backbone in EMA; the geometry is symmetric in both phases. Therefore, we are mapping an asymmetric theory (DEM) onto a symmetric theory (EMA).

We begin by choosing a fixed m which defines  $\epsilon(\phi)$  through the DEM solution  $\epsilon = \gamma \epsilon_1$ , where  $\gamma = (1 - \phi)^m$ .

TABLE I. Four examples of variable m and the corresponding DEM solutions for  $\epsilon_2 = 0$  and  $\phi = f_2$ .

<i>m</i> (φ)	$\epsilon(\phi)/\epsilon_1$
$m_0/(1-\phi)$	$\exp[-m_0\phi/(1-\phi)]$
$m_0+(m_1-m_0)\phi$	$(1-\phi)^{m_1}\exp[(m_1-m_0)\phi]$
$1/[m_0^{-1}+(m_1^{-1}-m_0^{-1})\phi]$	$\left[\frac{m_1(1-\phi)}{m_0\phi+m_1(1-\phi)}\right]^{m_1}$
$\frac{3}{2+\phi}$	$2\left(\frac{1-\phi}{2+\phi}\right)$

The spheroidal  $L(\phi)$  of EMA is then found by substituting for  $\gamma$  in Eq. (8). The equation for L is then

$$(1-\phi)[(1-\phi)^{m}-1)]\left(\frac{1}{(1-L)(1-\phi)^{m}+L}+\frac{4}{(1+L)(1-\phi)^{m}+(1-L)}\right)+\phi\frac{5-3L}{1-L^{2}}=0.(29)$$

Equation (29) is a quartic in L. However, we can make some general conclusions about its solution. First, by expanding Eq. (29) about  $\phi = 0$  we obtain

$$L(\phi = 0) = \frac{1 + \left[ (2m - 3)(2m - 1/3) \right]^{1/2}}{2m}.$$
 (30)

The permissible range of m is  $m \ge 3/2$ , which means that L (0) increases monotonically from 1/3 to 1 as m increases from 3/2 to  $\infty$ . Similarly, as  $\phi \rightarrow 1$ , Eq. (29) yields

$$L \sim (1 - \phi)/5$$
,  $\phi \rightarrow 1$ .

Thus, the EMA grains are oblate for small values of  $\phi$  but become prolate as  $\phi \to 1$ . The latter result is obvious from Figs. 1 and 2, since oblate grains have a maximum percolation threshold at 0.8, while prolate grains can have percolation at unity (needles). Thus, for  $\phi > 0.8$  the grains must be prolate and  $L(\phi) < L_c(\phi)$ , where  $L_c(\phi)$  is the value of L which gives a percolation threshold at  $\phi$ . It follows from Eq. (7) as

$$L_c = \{(9\phi - 4) - [(9\phi - 4)^2 - 12(1 - \phi)]^{1/2}\}/6, \quad (31)$$

and as  $\phi \rightarrow 1$ ,  $L_c = (1 - \phi)/5 + 0[(1 - \phi)^2]$ .

We have analyzed the solution to Eq. (29) for  $\phi$  almost zero and almost unity. For arbitrary  $\phi$  and m>3/2, there does not always exist a solution, see Figs. 1-3. This happens if the curve  $\gamma=(1-\phi)^m$  goes above the maximum possible  $\gamma$  of EMA, which was discussed in Sec. II. There is thus a minimum value of m below which Eq. (29) does not have a solution for all  $\phi$ . We note that for  $m=\log(3)/\log(9/5)$ , the DEM curve intersects and crosses the L=0 EMA curve at  $\phi=4/9$ . Therefore, the minimum m is greater than 1.87. Numerical computation shows the minimum value of m to be 1.89957.... We have plotted  $L(\phi)$  in Fig. 4 for several values of m greater than the minimum. The striking feature of each  $L(\phi)$  is that it suffers a jump from oblate to prolate at some value of  $\phi$  which increases with m. The strength of the

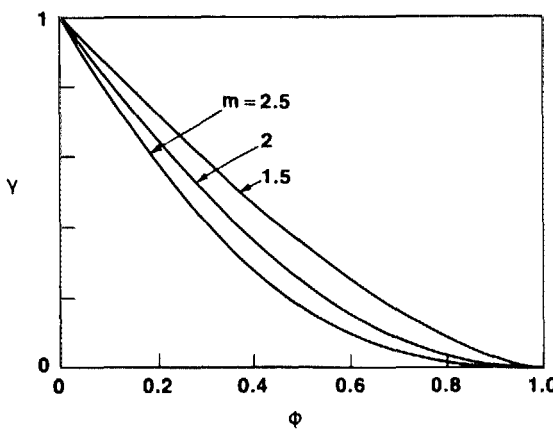


FIG. 3. DEM solution for conductor-insulator composite,  $\epsilon_2 = 0$ ,  $\epsilon = \gamma \epsilon_1$ , for 3 values of m from Eq. (25).

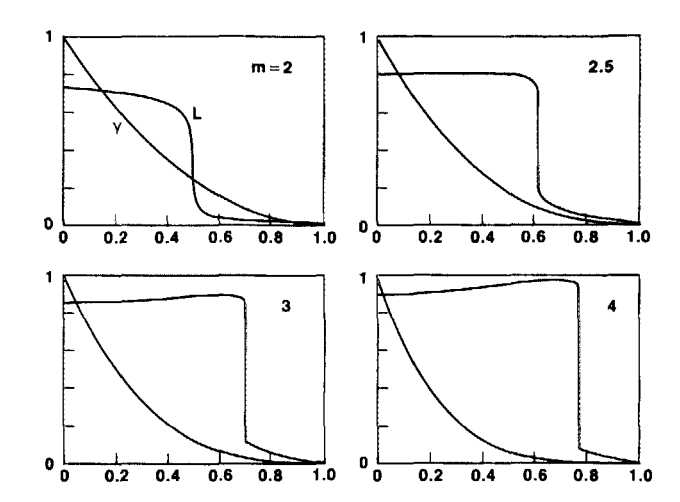


FIG. 4. The DEM solution and the corresponding L of EMA for the conductor-insulator composite,  $\gamma = \epsilon/\epsilon_1$ .

discontinuity or jump also increases with m. An understanding of the discontinuity follows from Figs. 1–4. Consider for example the m=2.5 curve in Fig. 3. As  $\phi$  increases from zero, this curve first stays close to the  $L\cong 0.8$  curve of Fig. 2. However, a critical point is reached when the DEM curve intersects the uppermost curve of Fig. 2 at  $\phi \cong 0.6$ . At this point, there is no oblate EMA curve with which the DEM curve can intersect, and so it must "jump" to a prolate EMA curve. Mathematically, the oblate and prolate EMA define two different branches which intersect along the L=1/3 curve. The point at which L "flips" from oblate to prolate in Fig. 4 is the point at which the DEM curve intersects the congruence of oblate EMA curves. The congruence is found by solving simultaneously Eq. (8) and its derivative with respect to L:

$$(1 - \phi)(\gamma - 1)^{2} \left( \frac{1}{[(1 - L)\gamma + L]^{2}} - \frac{4}{[(1 + L)\gamma + (1 - L)]^{2}} \right) + \phi \frac{(3 - L)(3L - 1)}{[1 - L^{2}]^{2}} = 0.$$
(32)

One solution to these equations is L=1/3,  $\gamma=(2-3\phi)/2$  for  $\phi < 2/3$ . However, at  $\phi \simeq 0.45$ , another solution becomes possible. This is the required oblate congruence, shown in Fig. 5. It bifurcates from the EMA sphere solution and continues until  $\phi=0.8$ , with L increasing from 1/3 to 1 along it. The "flipping" points in Fig. 4 are given by the intersection of the oblate congruence with the DEM curves, see Fig. 5. We have plotted the flipping point as a function of m in Fig. 6. We note that it asymptotes at  $\phi=0.8$  as  $m\to\infty$ .

The above analysis indicates that the mapping of DEM onto EMA involves a rather pathological microgeometry in the latter. Now both EMA and DEM are realizable theories. They are each defined by an incremental dilute-concentration approach. This corresponds physically to a hierarchy of length scales in the composite, such that consecutive length scales are of different orders of magnitude. The major difference between EMA and DEM in this picture is that EMA is symmetric and DEM is not. In DEM, the conductor (material 1) is a backbone which always percolates. On the other hand, the percolation properties of EMA depend in a subtle

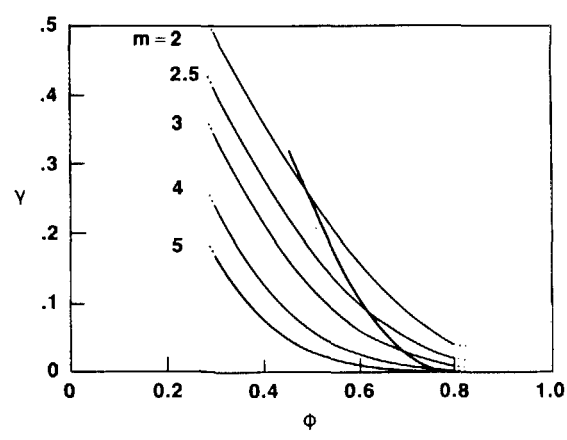


FIG. 5. The congruence of EMA curves (heavy line) and several DEM solutions. The discontinuity in  $L(\phi)$  occurs where the DEM curve intersects the congruence.

way upon the grain shape. The percolation threshold can be made arbitrarily close to zero by letting the grains be sufficiently needlelike. However, since in our present analysis both phases have the same shape, it is not intuitively obvious what effect the insulator grains have as the conductor grains become needlelike. The uncertainties over the shape of the nondominating phase are most critical at the flipping point when a sudden change from oblateness to prolateness in EMA corresponds to a continuous change in material properties as a function of volume fraction.

#### V. EFFECT OF INTERCHANGING THE PHASES

We now reverse the roles of the conductor and insulator, i.e., put  $\epsilon_1 = 0$ . The DEM solution then has the insulator as the backbone, or  $\epsilon(0) = 0$  in Eq. (12). The result is therefore  $\epsilon = 0$  for  $\phi < 1$ . Is the same result obtained when we exchange the phases in EMA with the  $L(\phi)$  that gave us DEM? The answer is no, because the EMA solution can be zero only if  $\phi < 1 - \phi_c(\phi)$ , where  $\phi_c$  is defined in Eq. (7). But we saw that  $\phi_c > 2/3$ , and so the EMA must give a nonzero result for  $1 - \phi_c(\phi) < \phi < 1$ . The solution in this range is  $\epsilon = \gamma \epsilon_2$ , where  $\gamma$  solves

$$\phi(\gamma - 1) \left( \frac{1}{(1 - L)\gamma + L} + \frac{4}{(1 + L)\gamma + (1 - L)} \right) + (1 - \phi) \frac{5 - 3L}{1 - L^2} = 0,$$
(33)

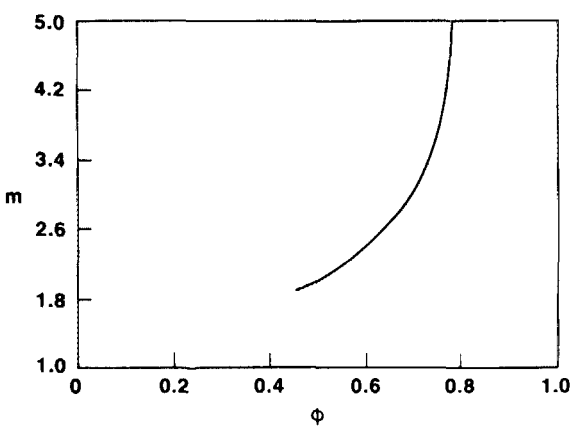


FIG. 6. The "flipping" point at which the EMA grains jump from oblate to prolate.

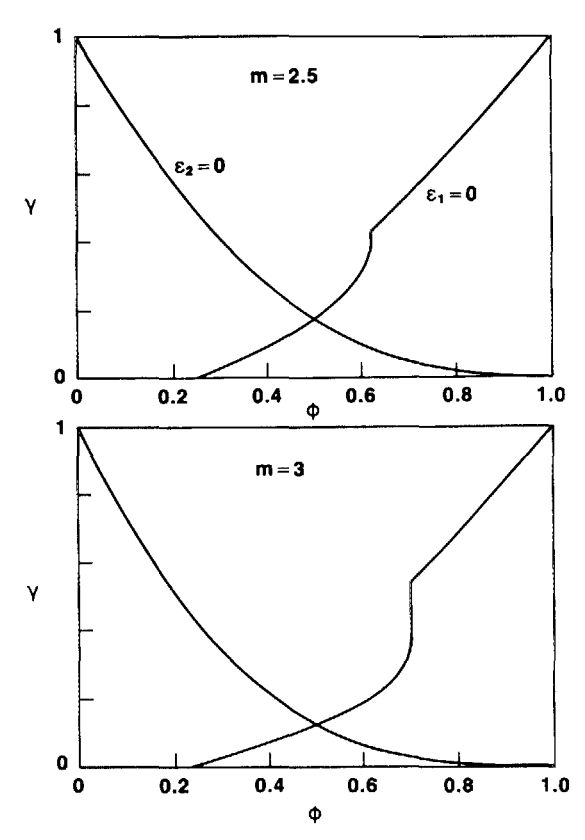


FIG. 7. The original DEM solution and the EMA solution when the roles of conductor and insulator are reversed.

with  $L(\phi)$  given by Eq. (29). We have plotted the EMA solution in Fig. 7 along with the solution for  $\epsilon_2 = 0$ . We note the discontinuity in  $\epsilon$  for the phase-exchanged solution.

It is not surprising that EMA does not reproduce DEM when the phases are interchanged. The DEM microgeometry is inherently unsymmetric while that of EMA is symmetric. If we had mapped EMA onto a symmetric theory, then the mapping would be conserved under the interchange of phases. For example, suppose that instead of DEM we had EMA with the grain shapes given by a distribution which is symmetric in the phases. We then proceed to find the equivalent EMA defined by  $L(\phi)$ , as we did for DEM. This mapping is automatically conserved when we interchange the phases, no matter what values  $\epsilon_1$  and  $\epsilon_2$  may have. Thus, we must be careful in comparing different effective-medium theories when one of the associated microgeometries is unsymmetric.

# **APPENDIX A: BOUNDS**

In general, it is possible to bound  $\epsilon$  within some region of complex space. These bounds have been discussed in detail by Bergman, <sup>17</sup> and may be improved upon if some statistical information is available. We consider the special case in which both  $\epsilon_1$  and  $\epsilon_2$  are real. Then  $\epsilon$  is also real and must lie between the Hashin–Shtrikman bounds, <sup>17</sup>

$$\epsilon_{-} \equiv h(\epsilon_{m}) < \epsilon < \epsilon_{+} \equiv h(\epsilon_{M}),$$
 (A1)

where  $\epsilon_m$  and  $\epsilon_M$  are the lesser and greater, respectively, of  $\epsilon_1$  and  $\epsilon_2$ . The function h(x) is

$$h(x) = \frac{2x\overline{\epsilon} + \epsilon_1 \epsilon_2}{2x + \epsilon_1 \epsilon_2 (\overline{1/\epsilon})},$$
 (A2)

1995

where the overbar denotes the volume-weighted average, e.g.,  $\bar{\epsilon} = f_1 \epsilon_1 + f_2 \epsilon_2$ . We note that the Hashin-Shtrikman bounds are equivalent to the Maxwell-Garnett approximation.

One may argue physically that since EMA and DEM both correspond to realizable isotropic composites, they must satisfy the Hashin-Shtrikman bounds. Here we present a mathematical proof. This provides a check on the realizability of the theories. We first show that the  $\epsilon$  of EMA always lies within the Hashin-Shtrikman bounds. The proof for spheres is straightforward since in this case Eq. (2) is equivalent to the equation

$$\epsilon = h(\epsilon). \tag{A3}$$

Now, for x > 0 we have h'(x) > 0 and h''(x) < 0. This implies that Eq. (A3) has only one positive root and it lies between  $\epsilon_-$  and  $\epsilon_+$ . When the grains are not spheres, we assume without loss of generality that  $\epsilon_1 > \epsilon_2$  and we let  $f_2 = \phi$ . Consider any value of  $\epsilon$  between  $\epsilon_1$  and  $\epsilon_2$ , say  $\epsilon = \beta$ . Then the upper bound  $\epsilon_+$  is equal to  $\beta$  at  $\phi = \phi_+$ , where

$$1 - \phi_{+} = \frac{3\epsilon_{1}(\beta - \epsilon_{2})}{(2\epsilon_{1} + \beta)(\epsilon_{1} - \epsilon_{2})}.$$
 (A4)

We consider the more general version of the EMA equation than Eq. (2) where the two components have different shapes. We have

$$\sum_{i=1,3} \frac{f_1(\epsilon - \epsilon_1)}{(1 - L_i^{(1)})\epsilon + L_i^{(1)}\epsilon_1} + \frac{f_2(\epsilon - \epsilon_2)}{(1 - L_i^{(2)})\epsilon + L_i^{(2)}\epsilon_2} = 0, \quad (A5)$$

where  $L_i^{(j)}$ , j=1,2 are the depolarization coefficients of material j. The EMA  $\epsilon$  of Eq. (A5) equals  $\beta$  at  $\phi = \phi_E$  where

$$\phi_E = \frac{\epsilon_2 S_1(\beta/\epsilon_1)(\epsilon_1 - \beta)}{\epsilon_2 S_1(\beta/\epsilon_1)(\epsilon_1 - \beta) + \epsilon_1 S_2(\beta/\epsilon_2)(\beta - \epsilon_2)}, \quad (A6)$$

where

$$S_j(x) = \sum_{i=1,3} \frac{1}{(1 - L_i^{(j)})x + L_i^{(j)}}, \quad j = 1 \text{ or } 2.$$
 (A7)

We have

$$\phi_{+} - \phi_{E} = \frac{(1 - \phi_{E})(\beta - \epsilon_{2})\epsilon_{1}M}{(\epsilon_{1} - \epsilon_{2})(2\epsilon_{1} + \beta)S(\beta/\epsilon_{1})}, \tag{A8}$$

where

$$\mathbf{M} = (1 + 2\epsilon_1/\epsilon_2)S_2(\beta/\epsilon_2) - 3S_1(\beta/\epsilon_1). \tag{A9}$$

We now show that M>0. First we note that  $S_2(x)$ , considered as a function of  $L_1$ ,  $L_2$ , and  $L_3$  subject to the condition  $L_1 + L_2 + L_3 = 1$ , is minimized by  $L_1 = L_2 = L_3 = 1/3$ . Also,  $S_1$  is maximized by putting one L equal to unity and the other two to zero. Thus,

$$M \geqslant \frac{9(1+2\epsilon_1/\epsilon_2)}{1+2\beta/\epsilon_2} - 3(1+2\epsilon_1/\beta) \equiv N(\beta),$$
 (A10)

with equality when the grains are spheres. The function  $N(\beta)$  is zero at  $\beta = \epsilon_1$  and  $\beta = \epsilon_2$  and is positive in-between. Therefore, M > 0, and so by Eq. (A8) we have that  $\phi_+ > \phi_E$ . This proves that the EMA  $\epsilon$  is bounded above by  $\epsilon_+$ . Similarly, it can be shown that  $\epsilon_-$  is a lower bound.

We will now show that the DEM  $\epsilon$  lies within the Hashin-Shtrikman bounds. Again let  $\epsilon_1 > \epsilon_2$  and  $\phi = f_2$ . Define  $\phi_D$  as the value of  $\phi$  at which the DEM  $\epsilon$  equals  $\beta$ . Thus,  $\phi_D$  follows from Eq. (13). We note that  $\phi_+$  of Eq. (A4) can be rewritten in the form

$$1 - \phi_{+} = \exp{-\int_{\beta}^{\epsilon_{1}} \frac{(\epsilon_{2} + 2\epsilon_{1}) d\epsilon}{(\epsilon - \epsilon_{2})(\epsilon + 2\epsilon_{1})}}.$$
 (A11)

Therefore,

$$\frac{1 - \phi_D}{1 - \phi_+} = \exp \int_{\beta}^{\epsilon_1} \frac{G(\epsilon) d\epsilon}{g(\epsilon, \epsilon_2)(\epsilon + 2\epsilon_1)},$$
 (A12)

where

$$G(\epsilon) = \frac{1}{3} \left( \sum_{i=1,3} \frac{\epsilon(2\epsilon_1 + \epsilon_2)}{(1 - L_i)\epsilon + L_i \epsilon_2} \right) - (2\epsilon_1 + \epsilon).$$
 (A13)

Now,  $G(\epsilon_2) = 0$  and  $\partial G/\partial \epsilon > 0$ , so  $G(\epsilon) > 0$ . Also,  $g(\epsilon, \epsilon_2) > 0$ . Therefore, the integrand of Eq. (A13) is positive which implies that  $\phi_+ > \phi_D$ . This proves that the DEM  $\epsilon$  is less than the Hashin-Shtrikman upper bound. Similarly, it can be shown that  $\epsilon$  is greater than the lower bound. We note that the above proof has not used the fact that  $L_1 + L_2 + L_3 = 1$ , but only that  $L_i > 0$ , i = 1,3.

<sup>1</sup>G. W. Milton, in *Physics and Chemistry of Porous Media*, edited by D. L. Johnson and P. N. Sen, AIP Conf. Proc. 107, 66 (1984).

<sup>2</sup>P. N. Sen, C. Scala, and M. H. Cohen, Geophysics 46, 781 (1981).

<sup>3</sup>A. N. Norris (unpublished).

<sup>4</sup>R. Landauer, J. Appl. Phys. 23, 779 (1952).

<sup>5</sup>D. A. Bruggeman, Ann. Phys. (Leipzig) 24, 636 (1935).

<sup>6</sup>M. Hori and F. Yonezawa, J. Phys. C. 10, 229 (1977).

<sup>7</sup>F. Yonezawa and M. H. Cohen, J. Appl. Phys. 54, 2895 (1983).

<sup>8</sup>W. E. Kohler and G. C. Papanicolaou, in *Multiple Scattering and Waves in Random Media* (North-Holland, New York, 1981), pp 199–224.

<sup>9</sup>J. G. Berryman, J. Acoust. Soc. Am. 68, 1809,1820 (1980).

<sup>10</sup>J. E. Gubernatis and J. A. Krumhansl, J. Appl. Phys. 46, 1875 (1975).

11G. W. Milton (unpublished).

<sup>12</sup>K. S. Mendelson and M. H. Cohen, Geophysics 47, 257 (1982).

<sup>13</sup>P. Sheng and A. J. Callegari, Appl. Phys. Lett 44, 738 (1984).

<sup>14</sup>P. Sheng and A. J. Callegari, in *Physics and Chemistry of Porous Media*, edited by D. L. Johnson and P. N. Sen, AIP Conf. Proc. 107, 144 (1984).

<sup>15</sup>R. McGlaughlin, Int. J. Eng. Sci. 15, 237 (1977).

<sup>16</sup>L. D. Landau and E. M. Lifshitz, Electrodynamics of Continuous Media (Pergamon, Oxford, 1960), p. 26.

<sup>17</sup>D. J. Bergman, Ann. Phys. 138, 115 (1982).